Send Orders of Reprints at reprints@benthamscience.net

Current Nanoscience, 2013, *9*, 173-182

Nitridation of Bulk Monocrystalline and Powdered Microcrystalline Gallium Arsenide Towards Cubic Gallium Nitride Nanopowders

Mariusz Drygas[a,*], Miroslaw M. Bucko[b] and Jerzy F. Janik[a]

AGH University of Science and Technology, [a]Faculty of Energy and Fuels, [b]Faculty of Materials Engineering and Ceramics; al. Mickiewicza 30, 30-059 Krakow, Poland

Abstract: Polished (111) surfaces of monocrystalline cubic gallium arsenide GaAs platelets and a powdered microcrystalline form of GaAs were nitrided towards gallium nitride GaN under a flow of ammonia at temperatures in the range 600-900 °C for one to several tens of hours. The progress of nitridation was followed mainly by grazing incidence X-ray diffraction GIXD and powder X-ray diffraction XRD. Morphology changes were examined with scanning electron microscopy supplemented with energy dispersive analysis SEM/EDX. Thermogravimetric and differential thermal analyses TGA/DTA were used to evaluate a thermal stability of the GaAs substrate. The substrate/temperature/time related interplay in the formation of the cubic and hexagonal GaN polytypes from cubic GaAs and conditions favoring the metastable cubic GaN polytype are delineated.

Keywords: Chemical synthesis, nitrides, crystal symmetry, nanostructures.

1. INTRODUCTION

Gallium nitride GaN has been considered for many advanced applications in modern electronics. It is a wide bandgap semiconductor (3.4 eV for hexagonal structure) showing high chemical and thermal resistance. With other III-V nitrides like hexagonal AlN and InN it forms crystalline solid solutions of a tailored bandgap from 1.8 to 6.2 eV [1]. Other crucial properties of GaN include the strong piezoelectric (2-6 MV/cm) and exciton (>50 meV) effects, high breakdown voltage (*ca.* $2 \cdot 10^6$ V/cm), and significant carrier mobility ($2.7 \cdot 10^6$ cm/s) [2]. This set of properties makes it a material of choice for advanced UV/Vis emission devices and detecting systems (*e.g.*, lasing and LED emission in blue), FET transistors working at high temperatures, phototovoltaic systems, fuel cells, high-density memory carriers, and many other key applications [3].

Under ambient conditions gallium nitride is found in two crystalline polytypes, *i.e.*, wurzite-type hexagonal h-GaN (P63mc, #186) and zinc blende-type cubic c-GaN (F43m, #216). It is worth to note that nanocrystalline powders of GaN in the low nanosized range exhibit heavily defected structures best described as the mixture of cubic and hexagonal close packed layers [4]. Many basic properties of these polytypes are quite similar while, for instance, differences encompass such values for the h-GaN and c-GaN as 3.4 and 3.2 eV at 300 K for the direct bandgap or 0.20 m_o and 0.13 m_o at 300 K for the effective electron mass, respectively. Not much is known about the thermal stability range for the cubic variety while the bulk hexagonal GaN as a nanopowder may survive several hours at 975-1000 °C and even at 1200-1300 °C as an epitaxial monocrystal [5]. Finally, the NaCl-type regular variety (Fm3m, #225) is known to be stable only under extremely high pressures [6].

Classic high-temperature syntheses starting mainly from metallic gallium and N_2/NH_3 nitriding agents result in the stable hexagonal structure [7]. Similarly, gallium halides [8a] and various oxygen-bearing gallium precursors [8b,c] yield the common h-GaN variety as do many typical metal organic chemical vapor deposition MOCVD processes [9].

Cubic GaN due to its somewhat different and often more advantageous properties than its hexagonal counterpart has become a subject of considerable interest in recent years [10]. The synthesis of c-GaN appears to be more challenging than that of h-GaN. For instance, thin films of cubic GaN were prepared on GaAs substrates *via* gas deposition techniques [11] and plasma-assisted nitridation [12]. Synthesis of free-standing c-GaN substrates grown by molecular beam epitaxy MBE was also reported [13]. Bulk crystalline c-GaN materials were made with an ammonothermal method utilizing various precursors [14]. Among the suitable methods those that dwell on topochemically-driven nitridation of phase-regular precursors require a special attention and the conversion of cubic gallium arsenide GaAs has become of special importance. For instance, plasma-assisted nitridation of GaAs at 700 °C under a pressure of 0.01 Torr resulted in a c-GaN layer while the pressure of 0.05 Torr yielded a mixture of c-GaN and h-GaN [15]. In another report, direct nitridation with ammonia at 700-1000 °C of powdered GaAs resulted in the mixtures of both phases of GaN and some residual GaAs [16a]. In order to achieve significant reaction progress, very long reaction times had to be applied at lower temperatures (80 h at 700 °C) or high temperatures had to be used close to the stability range of GaN (5 h at 1000 °C). However, in that report no detailed information about the starting powder except for its purity was provided. In this regard, the first known to us report on GaAs nitridation did not address the question of GaN polytype formation but concentrated on the feasibility of the arsenide to nitride conversion after all [16b]. In the related area, a topochemical reaction in the system nanocrystalline cubic GaP/N_2 was reported to yield at 500 °C a pure phase of nanocrystalline c-GaN or the phase in admixture with some metallic gallium and the nitride's average crystallite sizes in the range 16-22 nm [17].

Herein, reported is a study on the nitridation with ammonia of the (111) surfaces of the monocrystalline cubic GaAs substrates/platelets and a polycrystalline powder of the arsenide prepared by grinding of the monocrystal. The use of the platelets was aimed at investigating early stages of nitridation while both the powders and platelets were tested for conditions leading to the complete nitridation and high proportions of c-GaN. The progress of nitridation was followed for the surface-nitrided substrates by grazing incidence diffraction GIXD and for the powders and completely nitrided platelets by conventional powder XRD. Morphology of products was examined with scanning electron

*Address correspondence to this author at the AGH University of Science and Technology, Faculty of Energy and Fuels, 30-059, Krakow, Poland; Tel/Fax: (+48) 12 617 25 77; E-mail: madrygas@agh.edu.pl

1875-6786/13 $58.00+.00

© 2013 Bentham Science Publishers

microscopy SEM/EDX. TGA/DTA under helium was used to evaluate a thermal stability of the GaAs substrate.

2. EXPERIMENTAL

2.1. Nitridation

Polished (111) monocrystals of GaAs in the form of *ca.* 0.5-0.6 mm thick platelets were of commercial quality (Institute of Electronic Materials Technology, Warszawa, Poland). Powdered samples were obtained by grinding some of the GaAs platelets by hand in an agate mortar. The resulting powders had particle sizes spanning from a few to a few hundred microns (SEM observations) and, therefore, were in the microcrystalline size range. Anhydrous ammonia of 99.999 % purity was used as a nitriding agent. A GaAs sample, *i.e.*, either an individual platelet of *ca.* 5x5x0.5 mm for surface nitridation or some 0.5 g of powder accompanied aside by a small platelet in the crucible for complete nitridation, were loaded in an alumina crucible which was placed in a quartz reaction tube that was then inserted into a tube furnace. After an initial 10 minute purge with an ammonia flow of 1 cm^3/sec, a furnace reactor was heated under the flow of ammonia at 5 °C/min to a selected temperature in the 600-800 °C range for the platelets and in the 700-900 °C range for the powders/platelets. Upon reaching a target temperature, the heating was continued for a preset time and, subsequently, the furnace was cooled down under ammonia to ambient temperature. A black mirror of deposited elemental As was seen on colder parts of the reaction tube.

2.2. Characterization

All nitrided powders and platelets were characterized by standard powder XRD analysis (X'Pert Pro Panalytical, Cu K_α source; $2\Theta = 20–80°$). After nitridation, the platelets retained their initial shape while becoming porous and brittle. Following the XRD determination, typically, the brittle platelets were ground by hand in an agate mortar and checked again by powder XRD. Each powder sample was placed in a metal support and pressed by applying a normal force and shear motion to make the surface of the powder mount smooth and flat. Average crystallite sizes were evaluated from Scherrer equation applying the Rietveld refinement method. For the evaluation, changes of the line profile parameters compared to a standard sample were utilized. Our standard was a poly-crystalline alumina sintered body with an average grain size over 5 μm subjected to stress relief annealing. The profile parameters depend on the instrument settings used for data collection and on the profile function used for the refinement. In our analysis, the full Voigt function was used to describe the profile of the measured diffraction lines. The total profile width is a convolution of the Gaussian profile part and of the Lorentzian profile part and these parts are combined numerically. In such a method, the full width at half-maximum (fwhm) is only one of several fitted parameters. In a few cases of patterns containing severely overlapped peaks for different phases, the crystallite sizes were estimated from the strongest low angle peaks. The problem of particle size estimations for nanocrystalline materials from XRD data is not unequivocal but we believe that the consistent procedures for data acquisition and analysis yield reasonable results for comparison purposes as elaborated in our recently published studies on GaN nanopowders [5]. For the partially nitrided platelets, phase composition of the samples was determined with the grazing incidence X-ray diffraction technique (GIXD) in the Bragg-Brentano geometry. The measurements were carried out at the angle of incidence equal 1°. X-ray diffraction patterns were recorded in a 2-theta range 10-90° with a step of 0.02° and acquisition time of 10 sec per step. SEM micrographs were acquired with a Hitachi Model S-4700 scanning electron microscope. TGA/DTA determinations were carried out on the TA-Instruments STA-SDT 2960 apparatus (alumina crucibles, helium UHP 5N, sample mass 50-80 mg, helium purge before determinations at 30 °C for 1 h, heating rate 10 °C/min). Table **1** includes sample names, reaction conditions, and weight losses during nitridation.

3. RESULTS AND DISCUSSION

The thermodynamic driving force for the conversion of GaAs to GaN *via* the overall nitridation reaction $GaAs + NH_3 \rightarrow GaN + AsH_3$ ($As + 3/2H_2$) resides in the relevant enthalpies of their formation, *i.e.*, -81.5 kJ·mol^{-1} [18a] and -129.3 kJ·mol^{-1} [18b], respectively. Despite its quite common occurrence and remarkable stability at room temperature, the less common cubic polytype of GaN (zinc blende structure), c-GaN, is metastable requiring either a kinetic reaction control or stabilization by suitable centers [19]. In this regard, some theoretical calculations yielded the total energy of c-GaN of merely 34 meV/unit formula higher than in the stable hexagonal wurtzite structure, h-GaN, rendering the formation of both phases plausible under typical experimental conditions [20]. The formation of c-GaN *via* nitridation from the common cubic polytypes of GaAs and GaP may, in principle, result from the advantageous topochemical relationship set up by the conversion of the initial cubic lattice *via* element V exchange under suitable conditions.

The experimental weight losses point out that all completely nitrided powders/platelets and those surface-nitrided platelets that were subjected to the highest applied temperatures of 750-800 °C underwent some easily detectable nitridation (Table **1**). In this regard, a theoretical weight loss for a complete conversion of GaAs to GaN is 42.1 wt%. This exact value was actually observed for powder B nitrided at 800 °C for 90 hours. In general, all remaining cases of the complete powder/platelet nitridation also resulted in very high conversion ratios. The magnitudes of weight losses for the partially/surface nitrided platelets are intentionally much lower, *i.e.*, 1.8 to 7.7 wt%, indicating incomplete and mostly surface-confined nitridation as will be discussed below. Despite small or insignificant weight losses, all platelets including samples 1-7 displayed on the otherwise black surface a characteristic for GaN brownish-yellow coloration. It is worth to point out that the GaAs platelets upon complete nitridation still assumed the initial shape in the product but they were not monocrystalline anymore but they consisted of GaN nanopowders in the aggregated form.

The XRD scans for the samples A, B, and C are shown in Figs. (**1**,**2**, and **3**), respectively, and the phase contents, average crystallite sizes, and estimated lattice constants are included in Table **2**. In this regard, the crystallite sizes calculated for h-GaN for the (002) and (100) diffractions are referred to the crystallite dimensions along the *c*-axis and perpendicular to it, respectively, pointing to a prevailing crystallite shape, whereas the size calculated from the (101) diffraction reflects more of an average grain size characteristics. The analysis of line broadness for the c-GaN polytype indicates that for all samples the crystallite dimen-sions are comparable for different diffractions and, therefore, the strongest (111) diffraction is used to provide a representative average crystallite size. The data agree qualitatively with the results reported in the earlier study on GaAs nitridation [16a].

Such a diffraction line shape is consistent with a very broad crystallite size distribution of a likely bimodal characteristics spanning both the nanosized range (broad line component) and microsized range (sharp line component). The average crystallite sizes are calculated from the fwhm of the overall broad line and, therefore, they estimate the dimensions of the smallest crystallites after all. It is also worth noting that the calculated crystallite sizes along the various orientations for the h-GaN polytype indicate that there is a significant crystallite texturing for the samples A-powder and C-powder (platelet-type crystallites) while a more or less equadimentional crystallite shape is suggested for the sample B-powder. As already mentioned, the line shape analysis of the diffraction lines for the c-GaN polytype is consistent with quite regularly shaped crystallites in all powders. Finally, the calculated

Table 1. Sample Organization and Nitridation Conditions (n/a – not applicable)

Sample		Temperature [°C]	Time [h]	Weight loss [%]
Surface-nitrided platelets	0 (pure GaAs)			
	1	600	1	< 1
	2		24	
	3		60	
	4	650	1	
	5		12	
	6	700	1	
	7		6	
	8	750	1	1.8
	9		2	2.5
	10	800	1	7.7
Completely nitrided powders and platelets	A-powder A-platelet	700	90	39.5 40.5
	B-powder B-platelet B-ground platelet	800	90	42.1 42.0 n/a
	C-powder C-platelet C-ground platelet	900	6	41.5 41.3 n/a

Table 2. Crystalline Phases and Average Crystallite Sizes in the Completely Nitrided Powders and Platelets A, B, and C (n/d – not Detected)

	c-GaN			h-GaN			ResidualGaAs
Sample	**Content [%]**	**Crystallite size [nm]**	**Lattice constant, *a* [Å]**	**Content [%]**	**Crystallite size [nm]**	**Lattice constants, *a* and *c* [Å]**	**Content [%]**
A-powder	82	D(111) = 36	4.512	17	D(100) = 44 D(002) = 4 D(101) = 4	3.189 5.203	1
A-platelet	37	D(111) = 98	4.513	63	D(100) = 49 D(002) = 21 D(101) = 22	3.197 5.204	n/d
B-powder	61	D(111) = 41	4.508	39	D(100) = 51 D(002) = 41 D(101) = 44	3.191 5.191	n/d
B-platelet	62	D(111) = 29	4.507	38	D(100) = 14 D(002) = 9 D(101) = 10	3.191 5.186	n/d
B-ground platelet	64	D(111) = 38	4.509	36	D(100) = 42 D(002) = 42 D(101) = 43	3.191 5.192	n/d

(Table 2) Contd....

	c-GaN			h-GaN			ResidualGaAs
Sample	**Content [%]**	**Crystallite size [nm]**	**Lattice constant, *a* [Å]**	**Content [%]**	**Crystallite size [nm]**	**Lattice constants, *a* and *c* [Å]**	**Content [%]**
C-powder	84.3	D(111) = 67	4.511	15.4	D(100) = 35 D(002) = 6 D(101) = 7	3.192 5.191	0.3
C-platelet	77	D(111) = 55	4.509	23	D(100) = 38 D(002) = 49 D(101) = 50	3.192 5.188	n/d
C-ground platelet	89	D(111) = 76	4.509	11	D(100) = 59 D(002) = 59 D(101) = 59	3.190 5.192	n/d

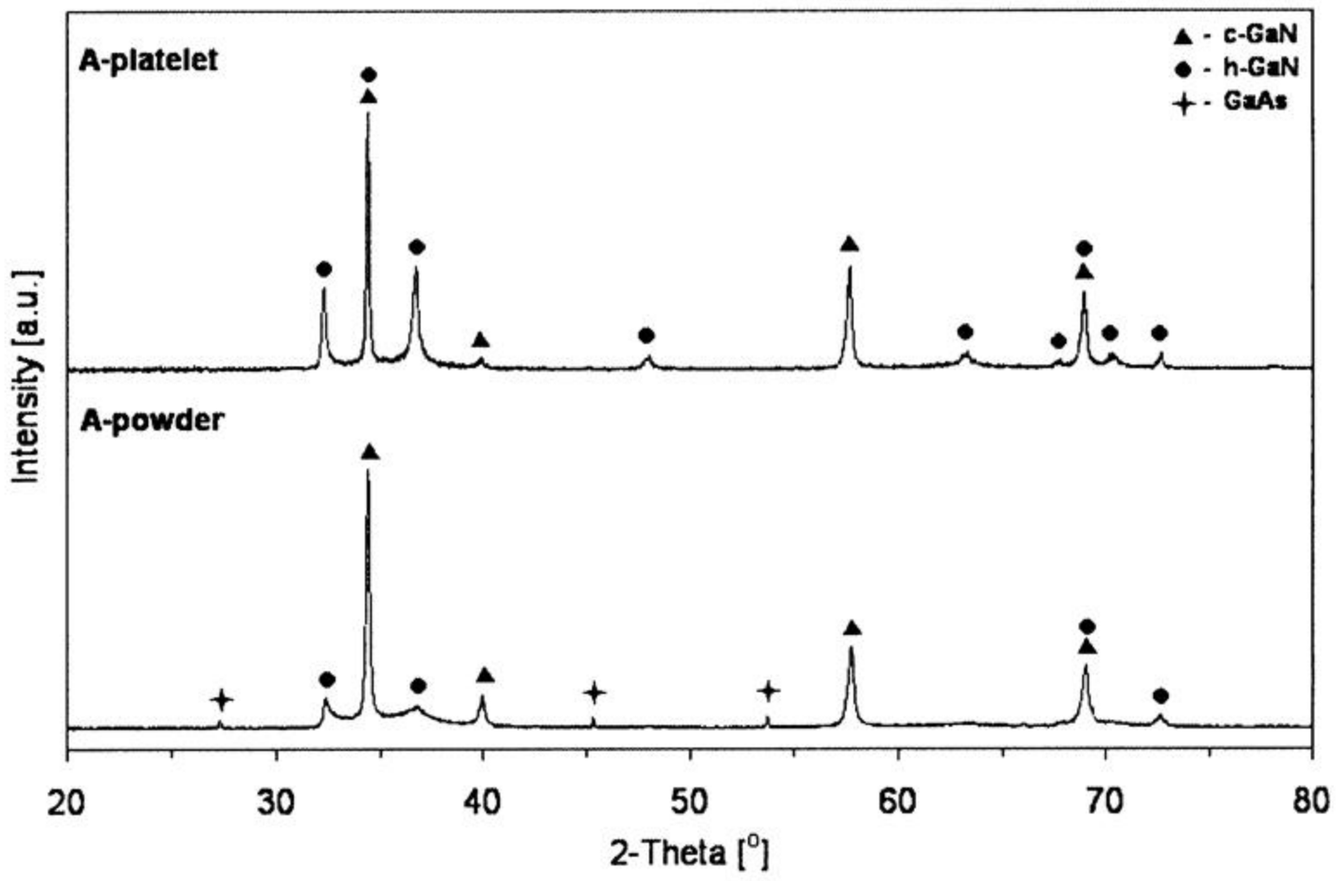

Fig. (1). XRD scans for nitrided samples A (bottom – powder, top – platelet).

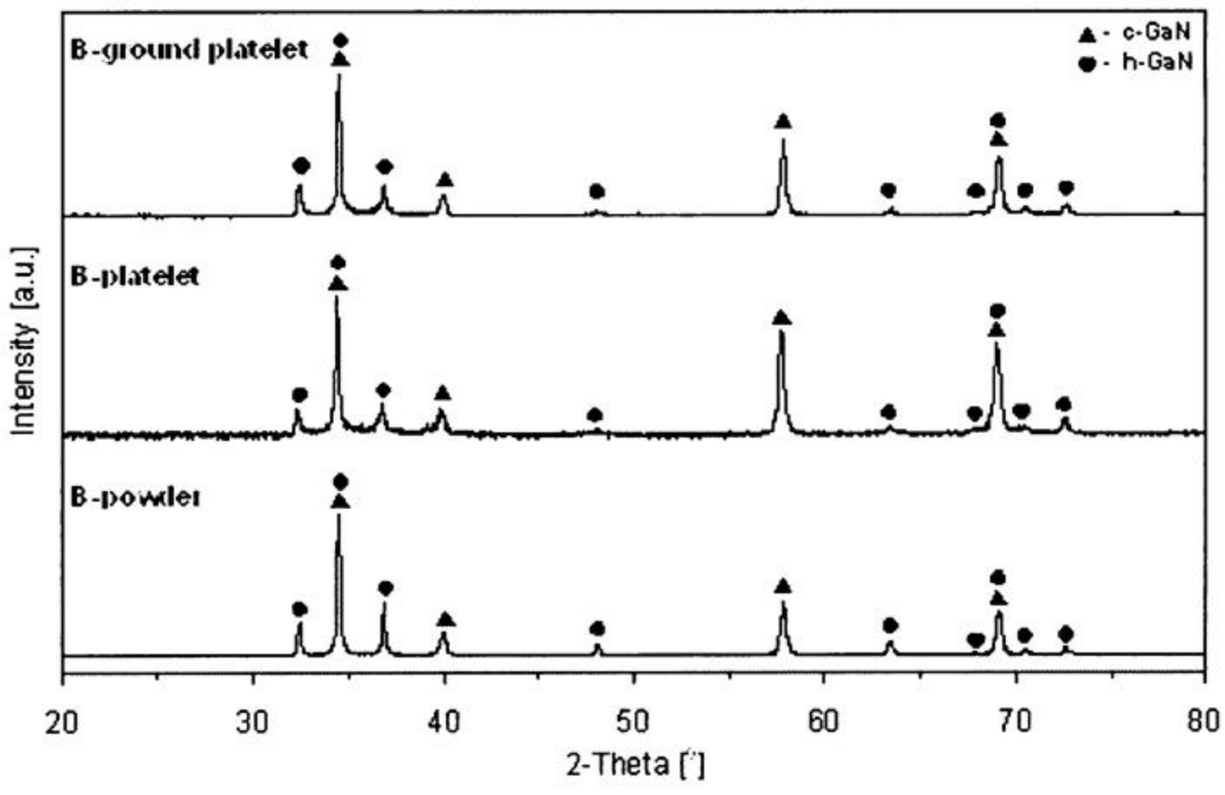

Fig. (2). XRD scans for nitrided samples B (bottom – powder, middle – platelet, top –ground platelet).

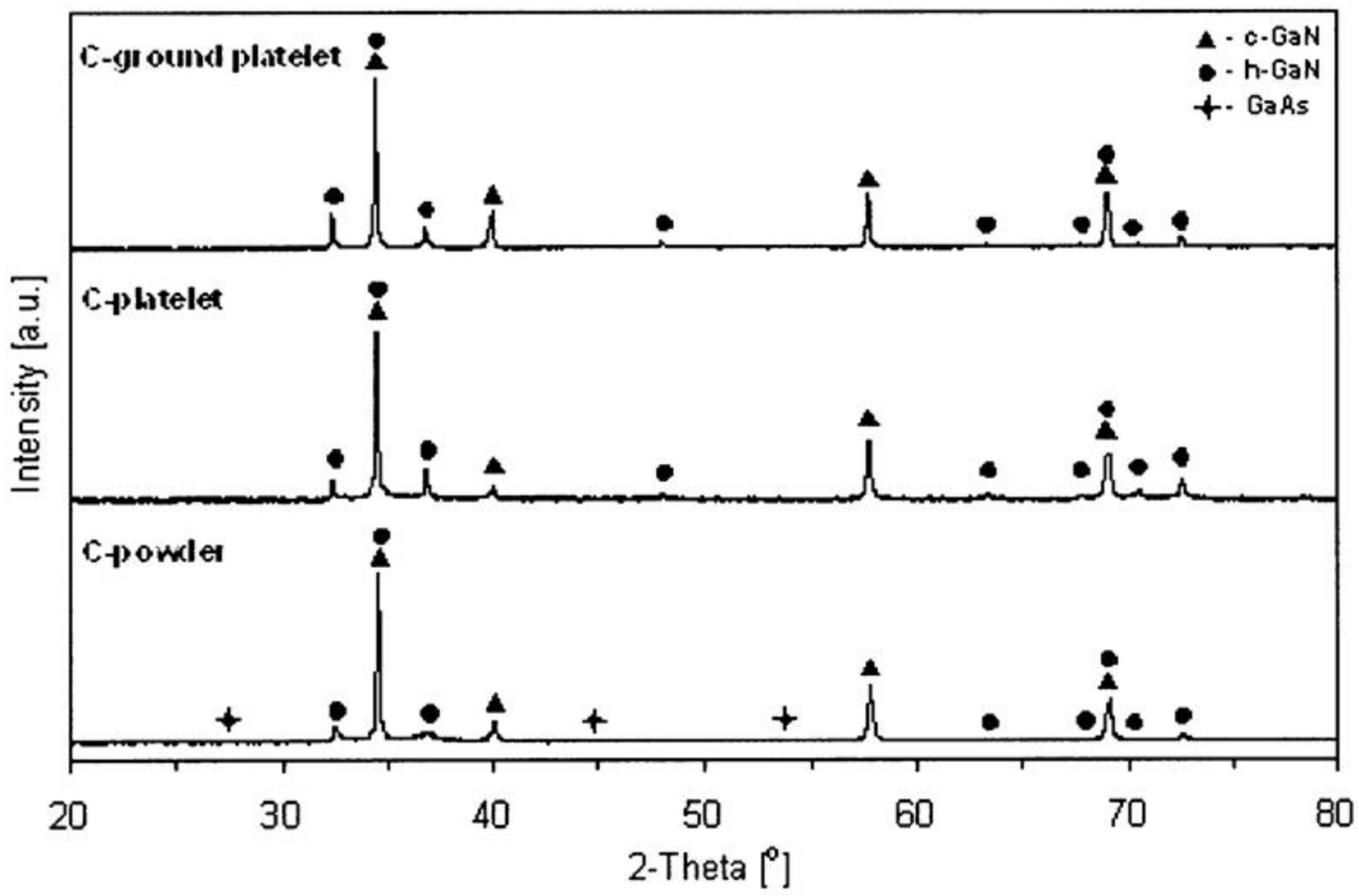

Fig. (3). XRD scans for nitrided samples C (bottom – powder, middle – platelet, top – ground platelet).

lattice constant for c-GaN, *a*, in all cases is within the range reported for this polytype, 4.506-4.518 Å [14a-c] while the *a* nad *c* lattice constants for h-GaN are typically a bit larger than the ones reported for not defected/well-crystalline h-GaN [22], *e.g.*, Ref. [22a] for a well-defined microcrystalline GaN: $a = 3.189(1)$ Å, $c = 5.185(5)$ Å.

Interestingly, in contrast to the powders none of the bulk and/or ground product platelets in this series of experiments is shown by XRD to contain any residual GaAs indicating the overall better nitridation conditions/outcome than found for the related powders. The proportions of both GaN polytypes are similar in the case of sample B-platelet and the related sample B-ground platelet (Fig. **2**) while the relative amount of c-GaN is found at a significantly higher level in the powdered sample C-ground platelet than in the initial bulk sample C-platelet (Fig. **3**). In this regard, the sample C-ground platelet showed the highest content of c-GaN obtained in this study, *i.e.*, 89 %. We want to point out that by grinding one averages out the surface and interior domains to get by XRD an overall average phase composition of the sample. On the other hand, the use of a platelet in such an experiment will, specifically, result in an average phase composition of the probed surface layer. Since the penetration depth of X-rays for both the samples B-platelet and C-platelet is similar, this suggests that the nitridation of the GaAs platelet at 900 °C for 6 hours (sample C) produces a surface layer enriched in h-GaN relative to the interior while the process at 800 °C for 90 hours (sample B) yields similar GaN phase compositions throughout the bulk and the surface.

The morphologies of all three powders appear to be similar. (Fig. **4**) exemplifies a typical texture of two of them, *i.e.*, completely nitrided powders B and C. The grains appear to preserve their basic irregular shape from grinding. Higher magnifications of grains (pictures on the right) resolve smaller constituent entities many of them sized below 100 nm that is consistent with the XRD estimations of the average crystallite sizes. Apparently, the product crystallites now form quite stable aggregates/agglomerates with increased porosity compared with the initial monocrystalline grains of GaAs. On the flat surface of one of the grains (bottom, righ-hand corner) originating, possibly, from a fragment of the initially polished (111) surface, textured parallel rows of quite uniformly-sized crystallites can be seen. This supports a conjucture that the crystallography-related topochemical circumstances play a significant role in the nitridation of GaAs.

The SEM images of all product platelets support a view that they consist of a rather thin and dense surface crust and an interior containing large globular crystallite agglomerates that appear to be aggregated in layers (Fig. **5**), low magnification pictures in the left-hand column). Higher magnifications of the surfaces indicate occasional regular texturing with parallel rows of quite uniformly shaped crystallites (Fig. **5**, middle column).

In sample A-platelet, there are interior regions containing well-shaped micron-sized hexagonal crystallites with tip-like ends (Fig. **5**, top row, right-hand side). The chemical circumstances and crystallite shape suggest here the likely growth from a liquid phase. Regarding this, our TGA/DTA study for a small platelet shows that GaAs starts to decompose to the elements with sublimation of arsenic at *ca.* 900 °C under helium (Fig. **6**) but the reducing conditions of the ammonia atmosphere in the nitridation study will likely lower this threshold temperature. This implies in all cases a certain degree of gallium arsenide decomposition with formation of liquid gallium (m.p. 29.3 °C), as no other liquid phases are anticipated in this system, followed by its *in situ* nitridation and crystallization of the GaN product. Since the nitridation of metallic gallium yields h-GaN, this mechanism seems to prevail in the case of A-platelet being responsible for the highest proportion of h-GaN among all the starting platelets in this series of experiment, *i.e.*, 63 % compared with 38 % and 23 % in the B-platelet and C-platelet, respectively. It is apparent when going from the A-platelet to C-platelet that the higher the nitridation temperature the lower is the content of h-GaN suggesting the GaAs decomposition pathway becoming less significant with increased temperatures. The prevailing crystallite shape in some of the large spheroidal aggregates in the sample B-platelet is of tetrahedral habit that is also typical for h-GaN (Fig. **5**, middle row, left and right-hand side images). These spherical features support the transient formation of liquid gallium metal as previously discussed. Such features are also seen in sample C-platelet (Fig. **5**, bottom row, left-hand side) while the crystallite habit here is different than previously described being now characteristic of hexagonal micro-multiplatelets (h-GaN) tightly admixed with rectangular blocky shapes (c-GaN).

Initial stages of nitridation of the smooth (111) surface of GaAs were also studied. As already mentioned, the compound starts to decompose under helium at 900 °C. At the same time, thermal dissociation of ammonia to reactive species including *in situ* formed nitrogen becomes significant at 600-700 °C. These were the

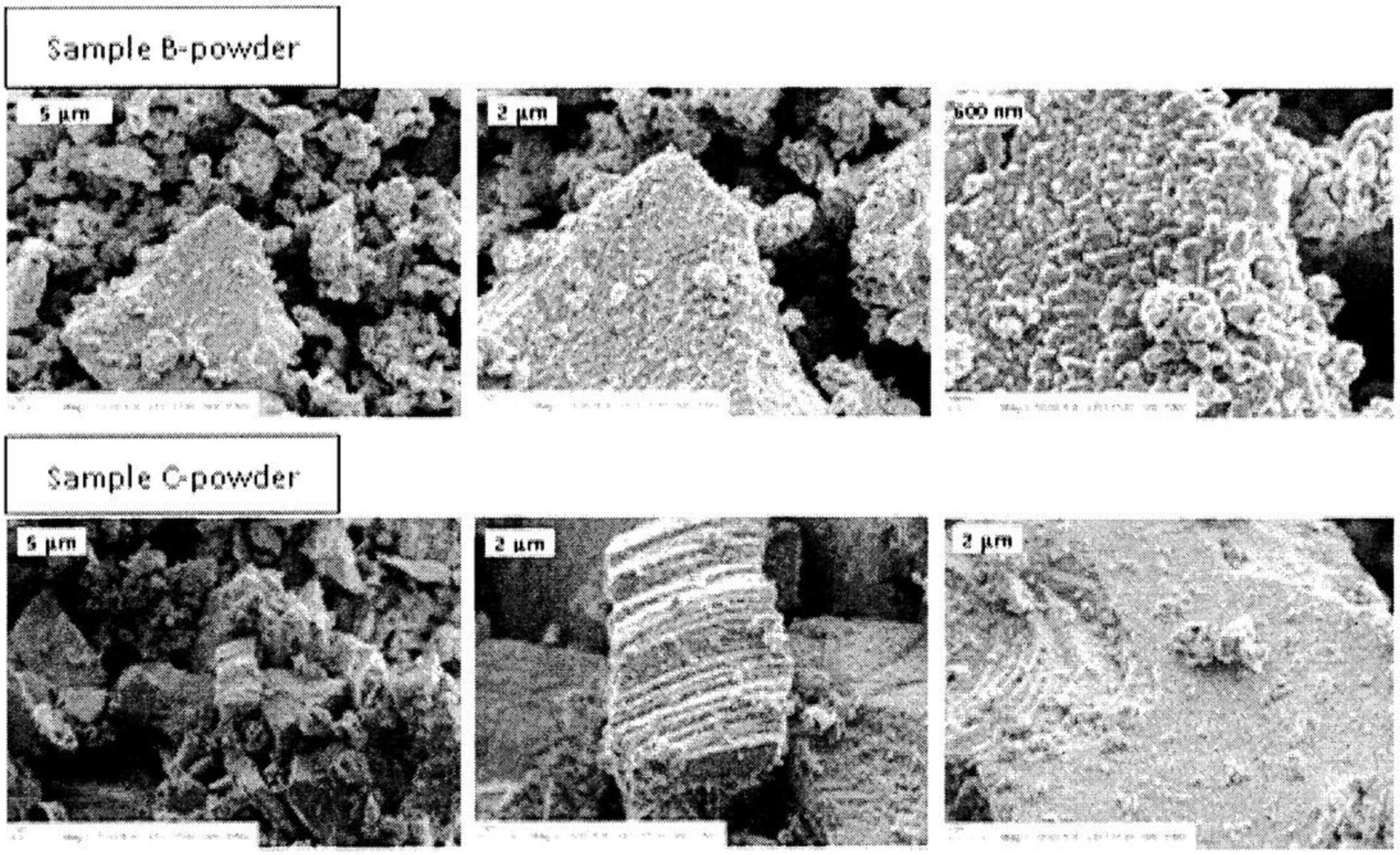

Fig. (4). SEM images of nitrided B-powder (top) and C-powder (bottom).

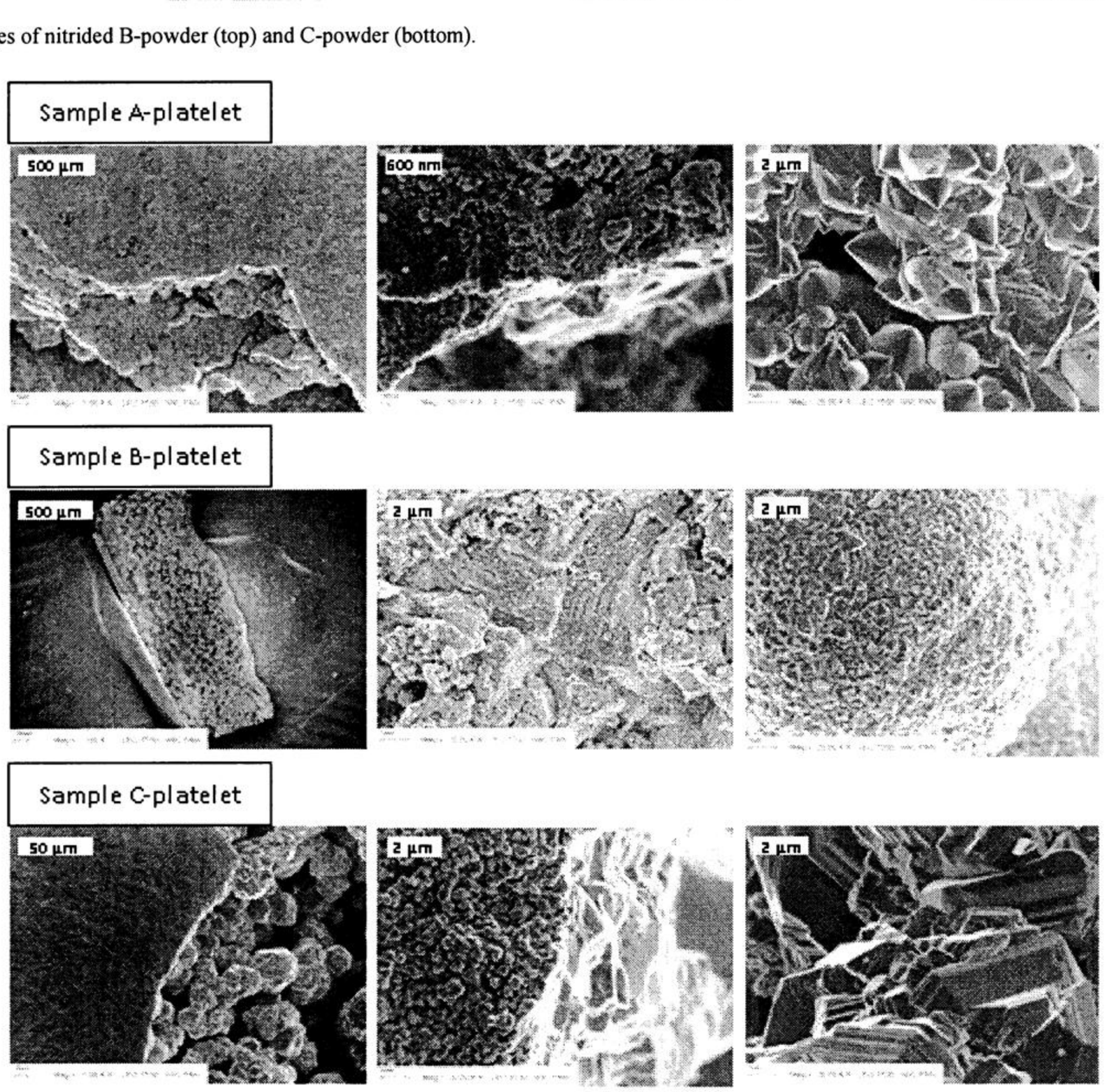

Fig. (5). SEM images of completetly nitrided platelets **A** (top), **B** (middle), and **C** (bottom).

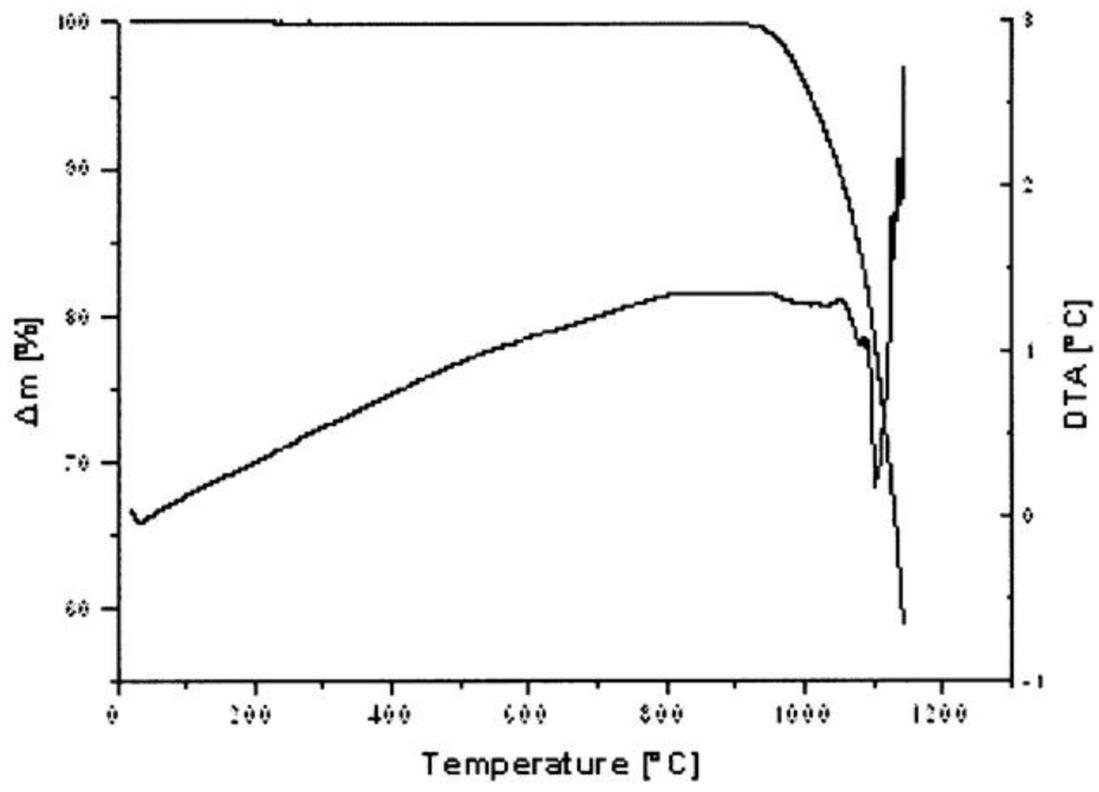

Fig. (6). TGA/DTA results for pure GaAs platelet (sample 0).

observations behind choosing the nitridation temperatures in the range 600-900 °C. Since we aimed at detecting a practical onset of nitridation, relatively shorter reaction times were tried compared with the experiments described earlier.

Fig. (**7**) shows the GIXD patterns including the reference sample 0 and the platelets nitrided at the lowest applied temperature of 600 °C for various times (samples 1, 2, and 3). Gallium nitride is detected on the surface mostly as a nanosized hexagonal polytype with traces of the cubic polytype after a 60-hour treatment at this temperature. Based on the specifics of GIXD determinations, all the remaining diffractions can be assigned to GaAs.

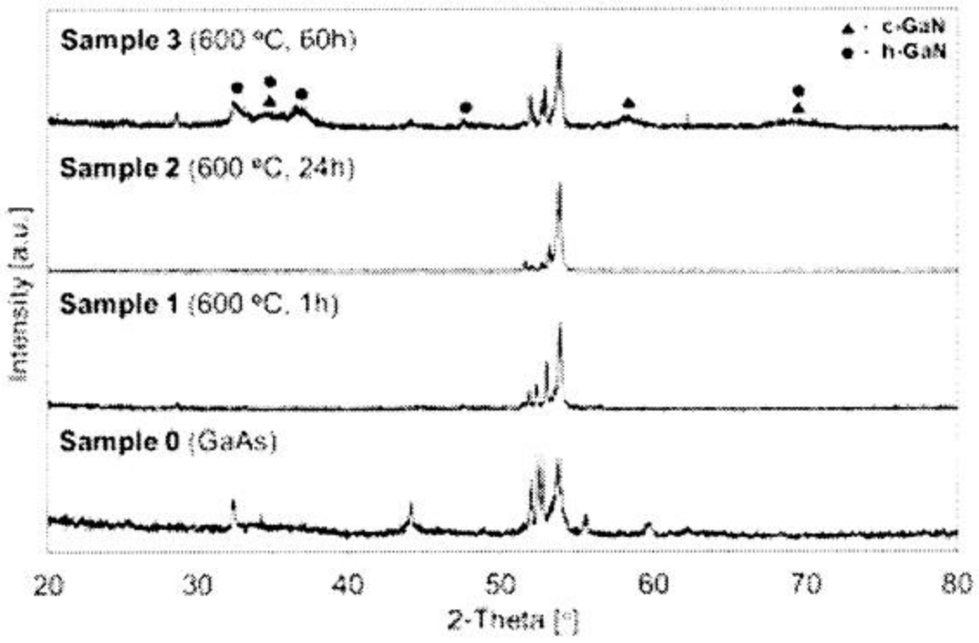

Fig. (7). GIXD diffraction patterns: reference sample 0 and samples 1, 2, and 3 nitrided at 600 °C.

Despite insignificant weight changes for samples 1-3 and no GaN phase detection by GIXD for samples 1 and 2 the SEM images of all the nitrided samples show distinct alterations of the surface as displayed in Fig. (**8**). Some pits appear already after a 1-hour nitridation and they grow with time. After a 60-hour reaction, numerous and quite uniform crystallites are seen that by EDX are confirmed to be GaN.

Nitridation at 650 °C for up to 12 hours does not produce detectable quantities of GaN at all (Fig. **9**). The surface morphology of samples 4 and 5 is similar to samples 1 and 2 showing the characteristic pits (Fig. **10**).

However, already after 1 hour at 700 °C (sample 6) there are indications about some h-GaN at the detection limits of the GIXD

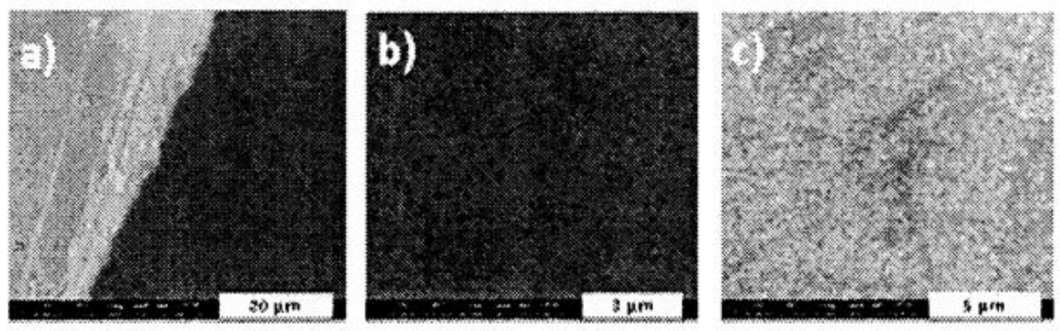

Fig. (8). Morphology of the initial and 600 °C-nitrided surfaces of GaAs platelets: **a**) initial GaAs platelet – sample 0; **b**) 600 °C, 1h - sample 1 (surface); **c**) 600 °C, 60 h – sample 3 (surface).

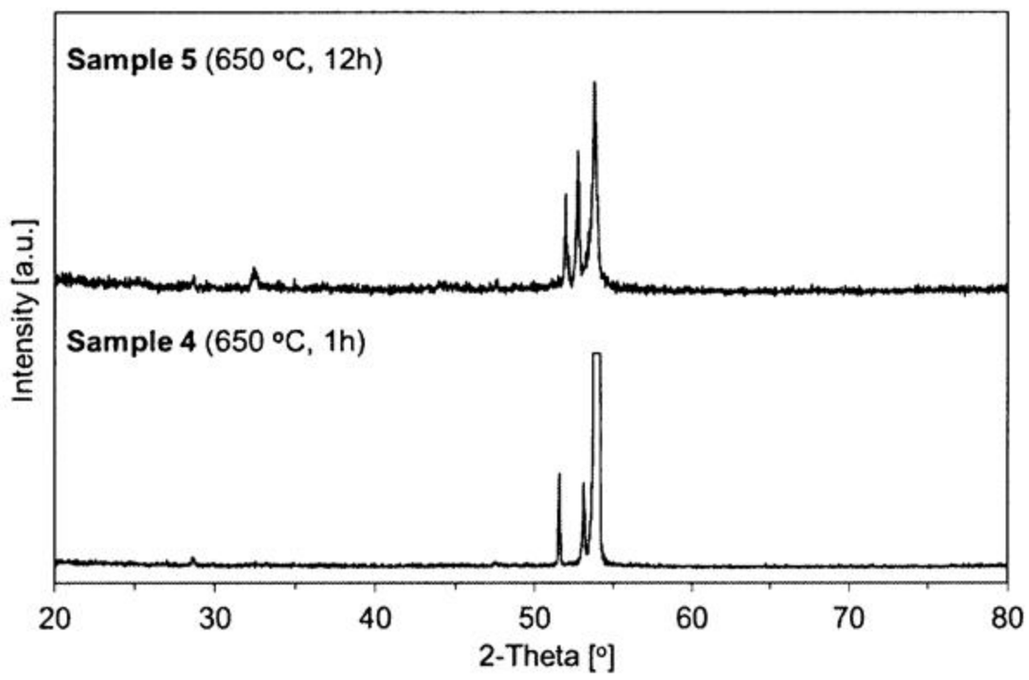

Fig. (9). GIXD diffraction patterns: samples 4 and 5 nitrided at 650 °C.

method while after 6 hours at this temperature (sample 7), the presence of the major nanocrystalline h-GaN admixed with a minor c-GaN component is unequivocal (Fig. **11**). The corresponding SEM images are shown in Fig. (**12**). Each sample is characteristic now of a mosaic of well-developed and quite deep pits that make the sample's chemically etched surface uneven and porous. EDX examination confirms gallium nitride present on both surfaces consistent with the GIXD data. The natural/original fracture edge of sample 7 (Fig. **12**, image **c**) shows relatively large droplets that by EDX are mostly elemental Ga suggesting that under local circumstances a decomposition of GaAs may take place with the formation of liquid Ga metal. This is consistent with the earlier results for the completete nitridation of GaAs at 700 °C where

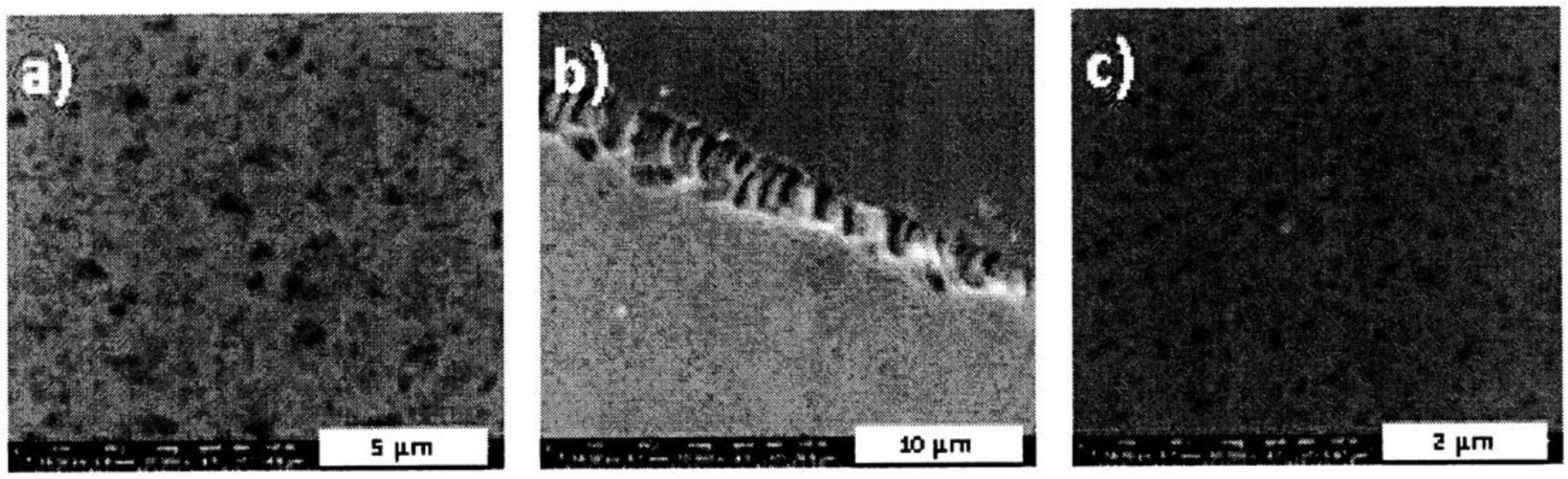

Fig. (10). Morphology of the 650 °C-nitrided surfaces of GaAs platelets: **a**) 650 °C, 1h - sample 4 (surface); **b**) 650 °C, 12 h - sample 5 (surface/fracture); **c**) 650 °C, 12 h - sample 5 (surface).

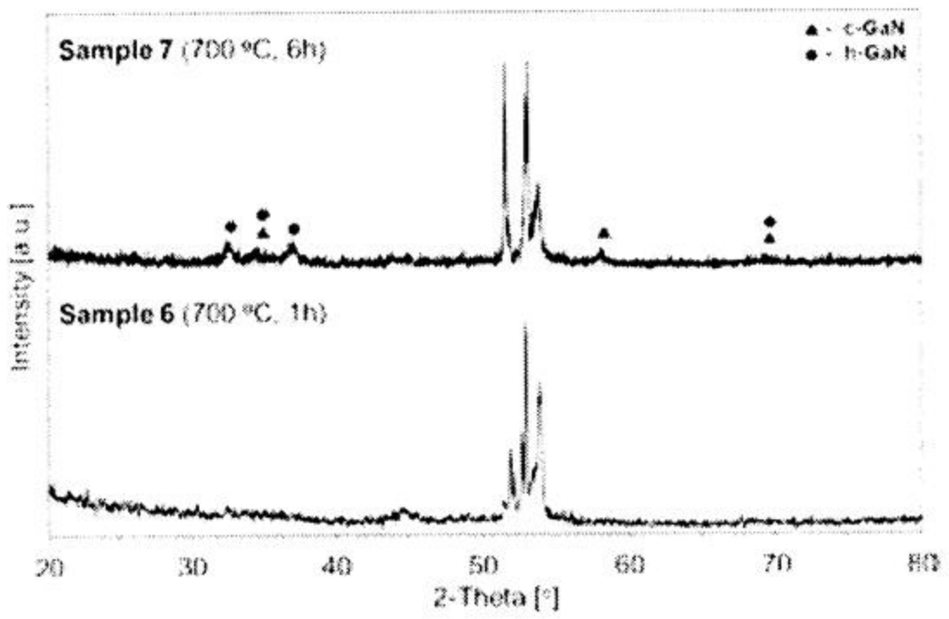

Fig. (11). GIXD diffraction patterns: samples 6 and 7 nitrided at 700 °C.

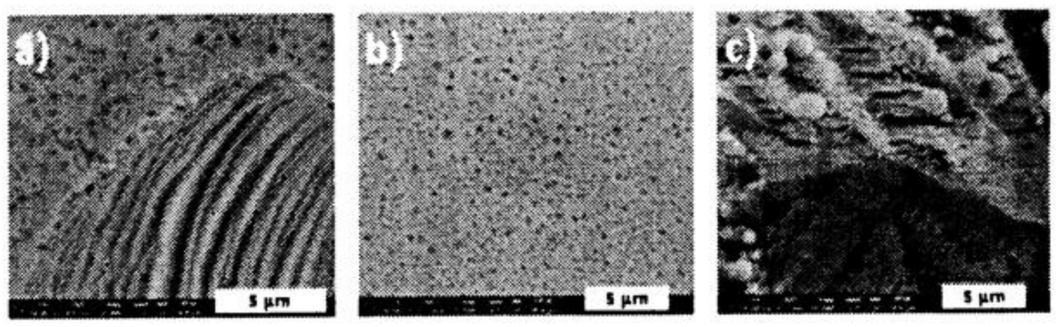

Fig. (12). Morphology of the 700 °C-nitrided surfaces of GaAs platelets: **a**) 700 °C, 1 h - sample 6 (surface/fracture); **b**) 700 °C, 6 h - sample 7 (surface); **c**) 700 °C, 6 h - sample 7 (fracture).

globular crystallite assemblages of GaN supposedly derived from the molten gallium were observed (*vide intra*).

In Fig. (**13**), compared are diffraction patterns for samples 8 and 9 that were nitrided at 750 °C for 1 hour and 2 hours, respectively, and for sample 10 after the 800 °C treatment for 1 hour. We want to recall that these conditions resulted in the detectable weight losses of the order of a few percent (Table **1**). All patterns show increasing with temperature and time cubic phase of GaN in addition to some h-GaN and GaAs from the substrate. The relative quantity of the latter in the surface layer is becoming smaller and smaller with temperature, especially, after the 800 °C nitridation. The 800 °C treatment results also in the highest proportion of c-GaN among all the samples in this series of experiments. The approximate relative amounts of both GaN polytypes in the surface layer probed in the GIXD experiments are shown in Table **3**.

The SEM images of samples 8-10 are included in Fig. (**14**). The well-developed porous surfaces with rather large pits sized below 1 µm are seen for all samples while, additionally, sample 10 from the highest applied nitridation temperature of 800 °C displays a few

Table 3. Relative Contents of c-GaN and h-GaN in the Surface-nitrided GaAs Platelets Estimated from GIXD data (n/d – not Detected)

Sample	c-GaN [%]	h-GaN [%]
1,2,4,5	n/d	n/d
3	< 1 (traces)	ca. 100
6	< 1 (traces)	ca. 100
7	< 1 (traces)	ca. 100
8	8	92
9	20	80
10	25	75

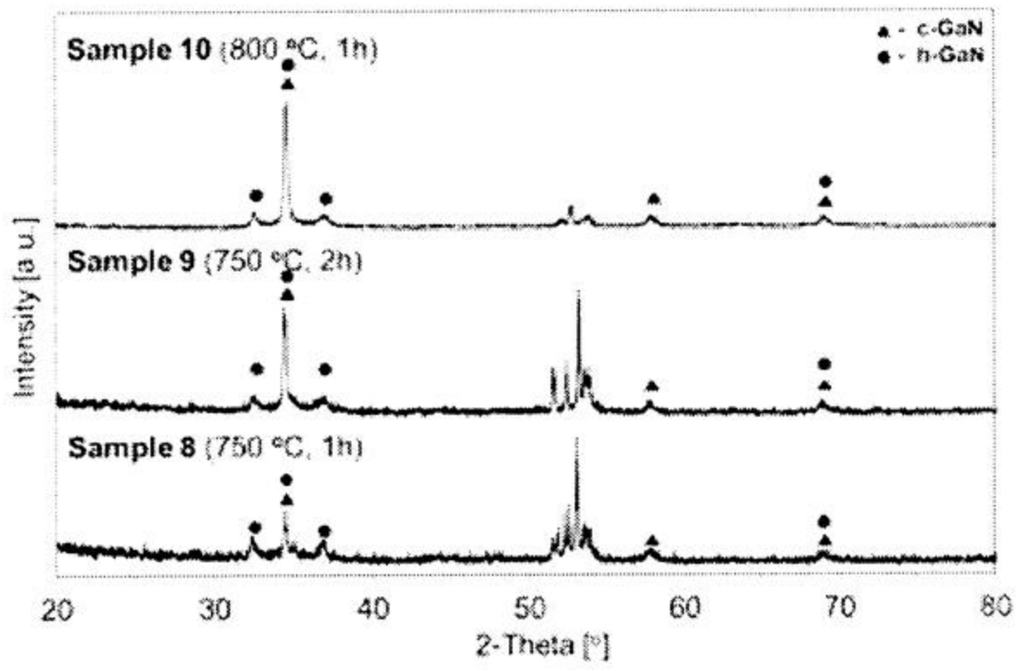

Fig. (13). GIXD diffraction patterns: samples 8 and 9 nitrided at 750 °C and sample 10 nitrided at 800 °C.

areas rich in small and large spheroidal particles. By EDX, these features are enriched in gallium suggesting GaAs side-decomposition under the applied conditions as already discussed for sample 7.

The GIXD data point out to the nitridation temperature as the crucial factor in the formation of cubic GaN on the (111) surfaces of the GaAs platelets and for the investigated reaction times and applied conditions the threshold temperature is around 750 °C. Below this temperature, *i.e.*, at 600-700 °C, even a several hour nitridation results in the major if not exclusive formation of

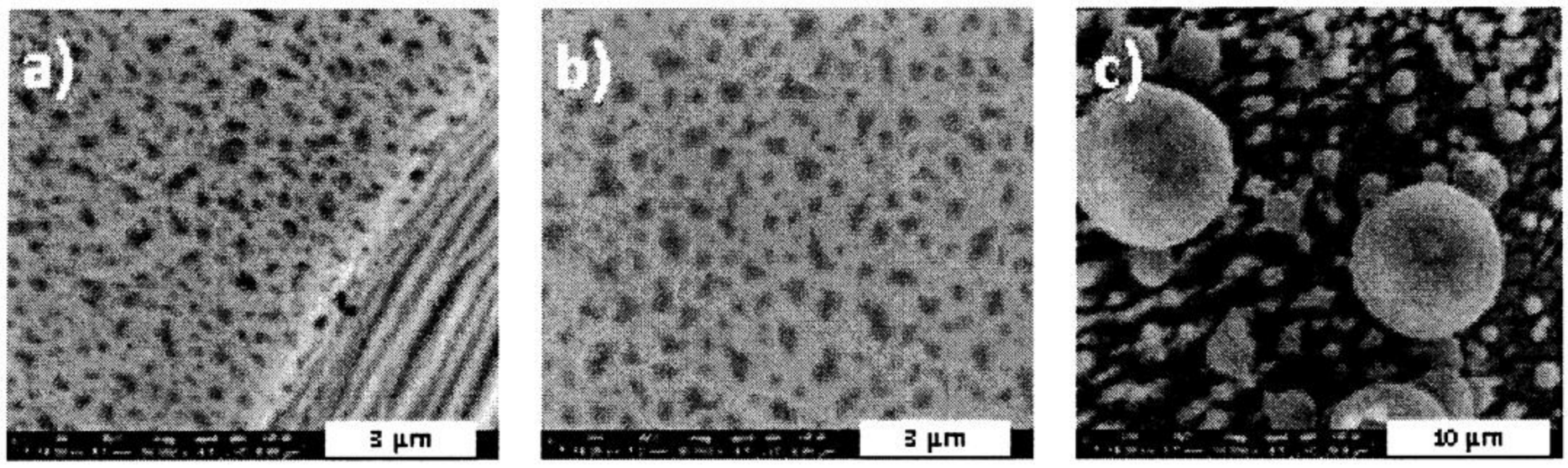

Fig. (14). Morphology of the 750 °C and 800 °C-nitrided surfaces of GaAs platelets: **a**) 750 °C, 1 h - sample 8 (surface/fracture); **b**) 750 °C, 2 h - sample 9 (surface); **c**) 800 °C, 1 h - sample 10 (area with spheres).

hexagonal GaN on the GaAs surface. At 750-800 °C, the formation of c-GaN is pronounced and its relative proportion seems to increase with nitridation time. It is to be recalled that for the sample A-platelet nitrided at 700 °C for 90 hours the prevailing product in bulk was c-GaN (63 %) while for the sample A-powder under the identical conditions the c-GaN polytype clearly dominated (82 %) (Table **2**). It appears, therefore, that the formation of c-GaN is diffussion/temperature controlled by the transfer of both nitrogen-in and arsenic-out species in this temperature range. It could also be enhanced by cubic lattice stabilisation by transient arsenic centers in the rather slow nitrogen-for-arsenic exchange.

The formation of h-GaN appears to take place, first, during the initial stages of heating GaAs under an ammonia flow to a target nitridation temperature and it is mainly confined to surface layers where cubic-related topochemistry does not play an important role, yet. In this regard, the passivated surface of GaAs is oxygen-rich and oxygen-bearing gallium compounds are known to yield on nitridation hexagonal GaN. Second, a decomposition side-reaction of GaAs associated with transient formation of small quantities of Ga metal also contributes to producing some h-GaN *via* the follow-up reaction of gallium with ammonia. Based on these observations, one can conclude that it will be extremely difficult in practice to achieve a complete nitridation of microcrystalline powders and/or bulk monocrystals of GaAs with an exclusive formation of c-GaN. However, the relative contents of c-GaN in the 80-90 % range are easily accessible by this route and further tailoring of experimental details (surface de-passivation, adjustments of heating rate and ammonia flow, *etc.*) will likely increase this level. Finally, not much is known about the thermodynamically favored conversion of the unstable c-GaN to the stable h-GaN at elevated temperatures and in the preceeding sections it was assumed that steady-state phase and recrystallization equilibria were in effect. To the best of our knowledge, the questions of a direct conversion of c-GaN to h-GaN and the thermal stability of c-GaN have not been yet experimentally explored and investigations in this area are in progress in our laboratory.

4. CONCLUSIONS

The nitridation with ammonia at 700-900 °C of the monocrystalline and powdered microcrystalline gallium arsenide GaAs results in the formation of mixtures of the major cubic polytype of gallium nitride GaN (rare, metastable variety) and the minor hexagonal polytype of the nitride (common, stable variety). The relative contents of cubic GaN at the 80-90 % level with average crystallite sizes in the range *ca.* 30-100 nm can conveniently be obtained by this route. The topochemical circumstances set up by the cubic lattice of the GaAs substrate are thought to be responsible, in principle, for its preferential nitridation/conversion to the metastable cubic GaN. Temperature-controlled diffusion conditions of the nitrogen-for-arsenic exchange in the initial cubic lattice of GaAs appear to be the crucial factor in enhancing this reaction pathway. Additionally, cubic lattice stabilisation by residual arsenic centers in the rather slow element V exchange process could also contribute. Side-decomposition of GaAs producing transient liquid Ga-metal domains as well as the presence of oxygen-rich passivating layers on GaAs are the likely reasons behind the formation of some stable hexagonal GaN. The question of the plausible conversion of the unstable cubic GaN to the stable hexagonal GaN at elevated temperatures and its impact on the experimentally observed relative contents of the polytypes need to be further explored.

CONFLICT OF INTEREST

The authors confirm that this article content has no conflicts of interest.

ACKNOWLEDGEMENTS

Research was supported by the Polish Ministry of Science and Higher Education, grant No. N N507 3676 33. Fruitful collaboration on some XRD data acquisition with Ewa Grzanka (Institute of High Pressure Physics, Polish Academy of Sciences, Warszawa, Poland) is appreciated.

REFERENCES

[1] Wua, J.; Walukiewicz, W.; Yu, K. M.; Ager III, J. W.; Li, S. X.; Haller, E. E.; Lu, H.; Schaff, W. J. Universal bandgap bowing in group-III nitride alloys. *Solid State Commun.*, **2003**, *127*, 411.

[2] Arakawa, Y. Progress in GaN-based quantum dots for optoelectronics applications. *IEEE J. Sel. Top. Quant. Elect.*, **2002**, *8*, 823.

[3] **a**) Nakamura, S. InGaN-based blue light-emitting diodes and laser diodes. *J. Cryst. Growth,* 1999, *202*, 290. b) Strite, S.; Morkoç, H. GaN, AlN, and InN: A review. *J. Vac. Sci. Technol. B,* **1992**, *10*, 1237. c) Oder, T. N.; Shakya, J.; Lin, J. Y.; Jiang, H. X. Nitride microlens arrays for blue and ultraviolet wavelength applications. *Appl. Phys. Lett.*, **2003**, *82*, 3692. d) Pearton, S. J.; Ren, F. GaN Electronics. *Adv. Mater.*, **2000**, *12*, 1571. e) Yun, F.; Chevtchenko, S.; Moon, Y. T.; Morkoç, H.; Fawcett, T. J.; Wolan, J. T. GaN resistive hydrogen gas sensors. *App. Phys. Lett.*, **2005**, *87*, No. 073507. f) Uthirakumar, P.; Ryu, B. D.; Kang, J. H.; Kim, H. G.; Hong, C. H. Impact of Nano-Texturing in GaN-based Light Emitting Diodes by Self-Assembled Silver Microspheres as Etch Mask. *Curr. Nanosci.*, **2011**, *7(6)*, 1000. g) Stavrou, V. N.; Veropoulos, G. P.; Markopoulos, A. Optical Properties of Manufactured III-Vs and II-VIs Short Wavelength Laser Structures. *Curr. Nanosci.*, **2010**, *5(3)*, 355.

[4] a) Hwang, J. W.; Campbell, J. P.; Kozubowski, J.; Hanson, S. A.; Evans, J. F.; Gladfelter, W. L. Topochemical Control in the Solid-State Conversion of Cyclotrigallazane into Nanocrystalline Gallium Nitride. *Chem. Mater.* **1995**, *7*, 517. b) Janik, J. F.; Wells, R. L. Gallium Imide, $\{Ga(NH)_{3/2}\}_n$, a New Polymeric Precursor for Gallium Nitride Powders. *Chem. Mater.*, **1996**, *8*, 2708.

[5] a) Drygas, M.; Olejniczak, Z.; Grzanka, E.; Bucko, M. M.; Paine, R. T.; Janik, J. F. Probing the Structural/Electronic Diversity and Thermal Stability of Various Nanocrystalline Powders of Gallium Nitride GaN. *Chem. Mater.*, **2008**, *20*, 6816. b) Drygas, M.; Bucko, M. M.; Olejniczak, Z.; Grzegory, I.; Janik, J. F. High temperature chemical and physical changes of the HVPE-prepared GaN semiconductor. *Mater. Chem. Phys.*, **2010**, *122*, 537. c)

Drygas, M. Janik, J. F. Modeling porosity of high surface area nanopowders of the gallium nitride GaN semiconductor. *Mat. Chem. Phys.*, **2012**, *133*, 932.

[6] Xu, F.; Xie, Y.; Zhang, X.; Zhang, S.; Shi, L. A benzene-thermal metathesis route to pure metastable rocksalt GaN. *New J. Chem.*, **2003**, *27*, 565.

[7] a) Johnson, W. C.; Parsons, J. B.; Crew, M. C. Nitrogen Compounds of Gallium. III. *J. Phys. Chem.*, **1932**, *36(7)*, 2651. b) Ejder, E. Growth and morphology of GaN. *J. Cryst. Growth*, **1974**,*2 2*, 44. c) Kamler, G.; Zachara, J.; Podsiadło, S.; Adamowicz, L.; Gębicki, W. Bulk GaN single-crystals growth. *J. Cryst. Growth*, **2000**, *212*, 39.

[8] a) Tavernier, P. R.; Clarke, D. R. Progress Toward Making Gallium Nitride Seed Crystals Using Hydride Vapor-Phase Epitaxy. *J. Am. Ceram. Soc.*, **2002,** *89*, 49. b) Wood, G. L.; Pruss, E. A.; Paine, R. T. Aerosol-Assisted Vapor Phase Synthesis of Gallium Nitride Powder. *Chem. Mater.*, **2001**, *13*, 12. c) Janik, J. F.; Drygas, M.; Stelmakh, S.; Grzanka, E.; Pałosz, B.; Paine, R. T. Tuning aerosol-assisted vapor phase processing towards low oxygen GaN powders. *Phys. Status Solidi A*, **2006**, *203*, 1301.

[9] a) Park, S. E.; Han, W. S.; H.G. Lee, B. O . Effect of native defects on electrical and optical properties of undoped polycrystalline GaN. *J. Cryst. Growth*, **2003**,*2 53*, 107. b) Tran, N. H.; Lamb, R. N.; Lai, L. J.; Yang, Y. W. Influence of oxygen on the crystalline-amorphous transition in gallium nitride films. *J. Phys. Chem. B*, **2005**, *109*, 18348.

[10] a) http://www.ioffe.rssi.ru/SVA/NSM/Semicond/GaN/bandstr.html. b) Yang, H.; Zheng, L. X.; Li, J. B.; Wang, X. J.; Xu, D. P.; Wang, Y. T.; Hu, X. W.; Han, P. D. Cubic-phase GaN light-emitting diode. *Appl. Phys. Lett.*, **1999**, *74*, 2498.

[11] a) Neumayer, D. A.; Ekerdt, J. G. Growth of Group III Nitrides. A Review of Precursors and Techniques. *Chem. Mater.*, **1996**, *8*, 9. b) Ambacher, O. Growth and applications of Group III-nitrides. *J. Phys. D-Appl. Phys.*, **1998**, *31*, 2653. c) Yasui, K.; Morimoto, K.; Akahane, T. Growth of GaN Films on Nitrided GaAs Substrates Using Hot Wire CVD. *Thin Solid Films*, **2003,** *30*, 174.

[12] Naddaf, M.; Hullavarad, S. S.; Ganesan, V.; Bhoraskar, S. V. Nitridation of porous GaAs by an ECR ammonia plasma. *Plasma Sources Sci. Technol.*, **2006**, *15*, 33.

[13] Foxon, C. T.; Novikov, S. V.; Stanton, N. M.; Campion, R. P.; Kent, A. J. Free-standing zinc-blende (cubic) GaN substrates grown by a molecular beam epitaxy process. *Phys. Status Solidi B*, **2008**, *245*, 890.

[14] For example, see: a) Purdy, A. P. Ammonothermal Synthesis of Cubic Gallium Nitride. *Chem. Mater.*, **1999**, *11*, 1648. b) Jouet, R. J.; Purdy, A. P.; Wells, R. L.; Janik, J. F. Preparation of Phase Pure Cubic Gallium Nitride, c-GaN, by Ammonothermal Conversion of Gallium Imide, {Ga(NH)3/2}n. *J. Cluster Sci.*, **2002**, *13*, 469. c) Jegier, J. A.; McKernan, S.; Purdy, A. P.; Gladfelter, W. L. Ammonothermal Conversion of Cyclotrigallazane to GaN: Synthesis of Nanocrystalline and Cubic GaN from $[H_2GaNH_2]_3$. *Chem. Mater.*, **2000**, *12*, 1003. d) Ehrentraut, D.; Hoshino, N.; Kagamitani, Y.; Yoshikawa, A.; Fukuda, T.; Itoh, H.; Kawabata, S. Temperature effect of ammonium halogenides as mineralizers on the phase stability of gallium nitride synthesized under acidic ammonothermal conditions. *J. Mater. Chem.*, **2007**, *17*, 886.

[15] Shimaoka, G.; Aoki, T.; Nakanishi, Y.; Hatanaka, Y.; Udagawa, T. Structure and optical properties of (0 0 1)GaAs surfaces nitrided in plasma-assisted NH_3 gas. *App. Surf. Sci.*, **2001**, *175-176*, 436.

[16] a) Jung, W. S.; Han, O. H.; Chae, S. A. Solid-state gallium NMR characterization of cubic gallium nitride prepared by the reaction of gallium arsenide with ammonia. *Mater. Chem. Phys.*, **2006**, *100*, 199. b) Addamiano, A. On the Preparation of the Nitrides of Aluminum and Gallium. *J. Electrochem. Soc.*, **1961**, *108(11)*, 1072.

[17] Gao, S. M.; Zhu, L. Y.; Xie, Y.; Qian, X. B. Formation of Cubic GaN Nanocrystals: A Study of the Thermal Stability of GaP Nanocrystals under Nitrogen. *Eur. J. Inorg. Chem.*, **2004**, *3*, 557.

[18] a) Kubaschewski, O.; Alcock, C. B. *Metallurgical Termochemistry*, 5th ed., Pergamon, New York, **1979**. b) Jacob, K. T.; Rajitha, G. Formation of Cubic GaN Nanocrystals: A Study of the Thermal Stability of GaP Nanocrystals under Nitrogen *J. Cryst. Growth*, **2009**, *311*, 3806.

[19] a) Kangawa, Y.; Akiyama, T.; Ito, T.; Shiraishi, K.; Kakimoto, K. Theoretical approach to structural stability of GaN: How to grow cubic GaN. *J. Cryst. Growth*, **2009**,*3 11*, 3106. b) Choi, E. A.; Chang, K. J. Stability of the cubic phase in GaN doped with 3d-transition metal ions. *Physica B*, **2007**, *401-402*, 319. c) Choi, E. A.; Kang, J.; Chang, K. J. Energetics of cubic and hexagonal phases in Mn-doped GaN: First-principles pseudopotential calculations. *Phys. Rev. B*, **2006**, *74*, No. 245218. d) Xu, M.; Liu, C. X.; Liu, H. F.; Luo, G. M.; Chen, X. M.; Yu, W. X.; Cui, S. F.; Li, J. H.; Chen, H.; Mai, Z. H.; Zhou, J. M.; Jia, Q. J.; Zheng, W. L.; Jiang, X. M. Thermal stability of cubic GaN film grown by molecular-beam epitaxy on GaAs(001). *Phys. Lett. A*, **2002**, *299*, 79.

[20] Mancera, L.; Rodriguez, J. A.; Takeuchi, N. Theoretical study of the stability of wurtzite, zinc-blende, NaCl and CsCl phases in group IIIB and IIIA nitrides. *Phys. Status Solidi B*, **2004**, *241*, 2424.

[21] Tachibana, H.; Ishido, T.; Ogawa, M.; Funato, M.; Fujita, S.; Fujita, S. Relation between GaAs surface morphology and incorporation of hexagonal GaN into cubic GaN. *J. Cryst. Growth*, **1999**, *196*, 41.

[22] a) Balkas, C. M.; Basceri, C.; Davis, R. F. Synthesis and characterization of high purity, single phase GaN powder. *Powder Diffr.*, **1995**, *10*, 266. b) Paszkowicz, W.; Podsiadło, S.; Minikayev, R. Rietveld-refinement study of aluminium and gallium nitrides. *J. Alloys Compd.*, **2004**, *382*, 100, and references therein.

Received: April 26, 2012 **Revised: November 22, 2012** **Accepted: December 3, 2012**